

MERLIN imaging of the maser flare in Markarian 348

E. Xanthopoulos & A.M.S. Richards

Jodrell Bank Observatory, University of Manchester, Macclesfield, Cheshire, SK11 9DL

ABSTRACT

MERLIN images of Mrk 348 at 22 GHz show H₂O maser emission at 0.02 – 0.11 Jy, within ~ 0.8 pc of the nucleus. This is the first direct confirmation that molecular material exists close to the Seyfert 2 nucleus. Mrk 348 was observed in 2000 May one month after Falcke et al. (2000) first identified the maser in single-dish spectra. The peak maser flux density has increased about threefold. The masing region is $\lesssim 0.6$ pc in radius. The flux density of radio continuum emission from the core has been rising for about 2 years. The maser-core separation is barely resolved but at the 3σ significance level they are not coincident along the line of sight. The masers lie in the direction of the northern radio lobes and probably emanate from material shocked by a jet with velocity close to c . The correlation between the radio continuum increase and maser flare is explained as arising from high level nuclear activity through a common excitation mechanism although direct maser amplification of the core by masers tracing a Keplerian disc is not completely ruled out.

Key words: masers - galaxies: individual (Markarian 348) - galaxies: nuclei - galaxies: Seyfert - radio lines: galaxies - radio continuum: galaxies

1 INTRODUCTION

Water maser emission has been detected from galaxies up to ~ 100 Mpc from Earth. These supermasers are hundreds of times more luminous than the brightest masers in star-forming regions in our own Galaxy (Cohen 1998). Such bright spectral lines are ideal targets for very long baseline radio interferometry with micro-arcsec accuracy and with $\lesssim 1$ km s⁻¹ velocity resolution. This is the only way to image distant galaxies directly on sub-pc scales.

H₂O supermasers are found exclusively in about 5% of type 2 Seyfert and LINER galaxies (Braatz et al. 1997). The unified scheme predicts that these active galactic nuclei (AGN) are obscured by a molecular torus viewed edge on. This provides high column densities for maser amplification (Kartje et al. 1999). Such masers have been used to measure the parameters of nuclear discs in Keplerian rotation (e.g. Miyoshi et al. 1995). It is less obvious why the selection effect applies to supermasers which appear to be associated with a jet instead of a circumnuclear disc (e.g. Claussen et al. 1998). These masers could originate from interstellar material shocked by the jet (Elitzur et al. 1992).

Falcke et al. (2000) reported the discovery of a very luminous H₂O maser in Mrk 348 during a radio flare of the AGN. Mrk 348 is a well studied Seyfert 2 at a redshift of 0.015 (Huchra et al. 1999), with broad emission lines in polarized light (Miller & Goodrich 1990). However its host

is an S0 galaxy at an angle of inclination of only $\approx 16^\circ$ (Simkin et al. 1987). Ground-based (Simpson et al. 1996) and HST (Falcke et al. 1998) imaging have revealed a dust lane crossing the nucleus. It has a high x-ray-absorbing column depth of $N_{\text{H}} = 10^{27.1}$ m⁻² towards the nucleus (Warwick et al. 1989). These observations suggest the presence of an obscuring torus in Mrk 348, but no molecular or HI absorption has been detected so far (Gallimore et al. 1999; Falcke et al. 2000).

In this paper all velocities are given relative to the local standard of rest (V_{LSR}) in the radio convention. The systemic V_{LSR} of Mrk 348 is $4435 \leq V_{\text{sys}} \leq 4480$ km s⁻¹ from HI emission line observations (Bottinelli et al. 1990) and imaging (Simkin et al. 1987). We adopt $H_0 = 75$ km s⁻¹ Mpc⁻¹, so Mrk 348 is at a distance of ~ 60 Mpc, where 1 mas = 0.29 pc.

What makes Mrk 348 stand out among Seyfert galaxies is its bright and variable inverted-spectrum radio nucleus (Unger et al. 1984). Jets at position angles (p.a.) 170° and 30° were observed with the EVN at 1.4 GHz (Neff & de Bruyn A G 1983) and MERLIN at 5 GHz (Unger et al. 1984). Halkides et al. (1997) first resolved the central part of Mrk 348, using the VLBA at 15 GHz, into two components separated by ~ 0.3 pc at p.a. $\sim 90^\circ$ to the larger 1.4 GHz jet. Ulvestad et al. (1999) measured the sub-relativistic separation rate of these two components at the same frequency. They also noted a rise in continuum flux from 120 to 570 mJy between 1997.10 and 1998.75. Using MERLIN we can detect mJy radio continuum with a surface

Contact e-mail: emily@jb.man.ac.uk, amsr@jb.man.ac.uk

brightness $\gtrsim 5 \times 10^4$ K and locate bright masers with sub-pc relative positional accuracy. We use this to investigate the relationship between the maser and continuum flares and their origins in the core or in a nascent jet.

2 OBSERVATIONS AND DATA REDUCTION.

We observed Mrk 348 on 2000 May 2 using MERLIN, which has a maximum baseline of 217 km, giving a beam size of 12 mas. In order to obtain images of Mrk 348 as rapidly as possible we observed for a single 17 hr run in the maximum 16 MHz bandwidth, which corresponds to a total velocity width of ~ 200 km s $^{-1}$ and only covers the red-shifted half of the line seen by Falcke et al. (2000) plus sufficient line-free channels for continuum subtraction. We observed Mrk 348 at a fixed frequency of $\nu_0 = 21891.6$ MHz alternately with phase reference source J0057+3021 for 4 and 2 min respectively. 3C273, which had a flux of 21.09 Jy at that time (Teräsranta, private communication), was observed for 40 min and used to set the flux scale for all sources.

Further data processing was performed using AIPS (Greisen 1994). We applied the instrumental corrections from the calibrators and the phase reference source solutions to Mrk 348. We then adjusted the data to a constant velocity, putting $V_{\text{LSR}} = 4641.6$ km s $^{-1}$ in channel 30 of 60 usable channels, with a separation of 3.37 km s $^{-1}$. We averaged all data for Mrk 348 and made a CLEAN map using natural weighting of the visibility data, which gave a beam size of 31 mas \times 21 mas.

The three CLEAN components (CC) above $3\sigma_{\text{rms}}$ from the initial map of Mrk 348 lay in a region 6 by 18 mas elongated north-south. We used these as a model for phase self-calibration, applied the solutions and examined the spectrum of Mrk 348. The complex visibilities were vector averaged in time channel by channel. The flux density increased noticeably with increasing frequency if we used the more southerly CC positions as the origin of phase. Fig. 1 shows the spectrum on the baselines to the Cambridge antenna using the mean position of the maser emission (Table 1) as the phase origin. The low-frequency end of the band appeared to be continuum only. We used the first 4.25 MHz of data for phase and amplitude self-calibration and applied the same corrections to the line-only data as we did for the continuum data.

The multi-channel Mrk 348 data were averaged over every 0.75 MHz and Fourier transformed to make a 20-channel total emission dirty data cube. The average of the first 4.50 MHz was subtracted pixel by pixel from the whole cube to leave a line-only dirty data cube which was CLEANED to produce a CLEAN line-only cube. The line-only dirty data cube was subtracted from the total emission dirty data cube and the result was CLEANED to give a continuum-only cube. We also made a CLEAN total emission cube.

We fitted 2D Gaussian components to emission above $3\sigma_{\text{rms}}$ in each channel of every CLEAN cube to determine the position and peak flux S_p . We also measured the position and flux density of components fitted to the total flux from Mrk 348 mapped using 15-MHz band-width prior to self-calibration and the 4.25-MHz bandwidth self-calibrated continuum map. The brightest continuum components was resolved after deconvolving the beam, so we could measure

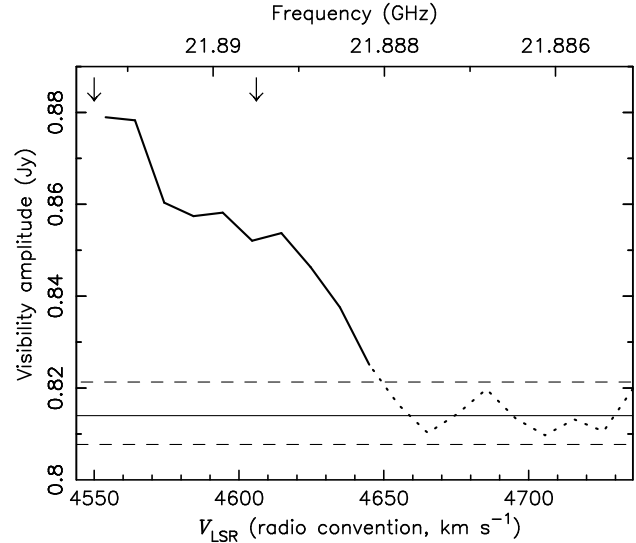


Figure 1. The total flux density of Mrk 348 in each channel. The arrows mark the frequencies of peaks observed by Falcke et al. (2000).

its FWHM s and the integrated flux S_i . The position and component size uncertainties (σ_{pos} , σ_s) are proportional to the beam-width divided by the signal-to-noise ratio allowing for the sparse baseline coverage (Condon et al. 1998; Richards et al. 1999).

All maps are presented in total intensity. The flux scale should have $< 10\%$ error but MERLIN only has 5 antennas operating at 22 GHz, and the sparse uv coverage means it is possible for extended continuum emission to appear brighter and more compact than it actually is, although the peak positions should be accurate. Moreover as only one side of the bandpass is line-free, errors in baseline subtraction or bandpass calibration may affect the maser flux measurements. The absolute position accuracy is ~ 50 mas, mostly due to uncertainty in the position of J0057+3021 (Wilkinson et al. 1998).

3 RESULTS

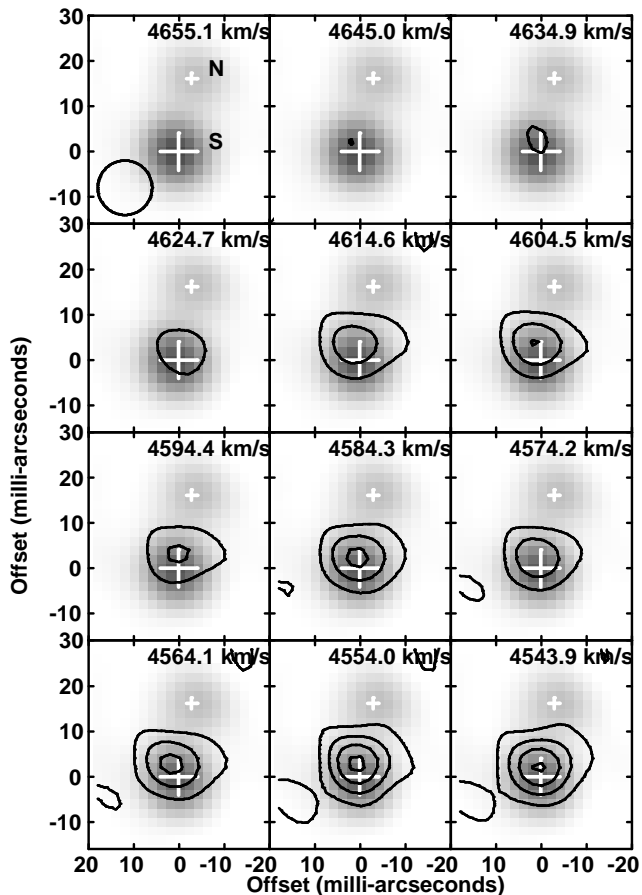
A single patch of maser emission was detected in 11 channel maps of the line-only data cube from 4543.8 to 4655.0 km s $^{-1}$, shown by the contours in Fig. 2. These are in linear multiples of $3\sigma_{\text{rms}}$. The grey-scale shows the continuum-only emission above $3\sigma_{\text{rms}}$. The continuum peaks are marked N and S and the white crosses show their positions, which agree in each channel to within 0.1 mas.

The positions and flux densities of the peaks are given in Table 1. The peak of the maser emission is consistently offset from the continuum peak; its mean position \bar{M} is 2.7 ± 0.7 mas north of S. The total angular size of the maser region is ≤ 3 mas and the individual components are unresolved. There is no significant systematic angular separation-velocity gradient greater than 2 mas in 111 km s $^{-1}$. S appears to be resolved, and was fitted with a component of 2.0 ± 0.2 mas FWHM and an integrated flux of 814 mJy giving a brightness temperature of $551 - 824 \times 10^6$ K. N is at a position angle of $-11^\circ \pm 2^\circ$ with respect to S.

The maps of continuum-only channels from 21884.35 to

Table 1. The positions and peak intensities S_p of the 22 GHz continuum and maser peaks in Mrk 348 N, S and \bar{M} .

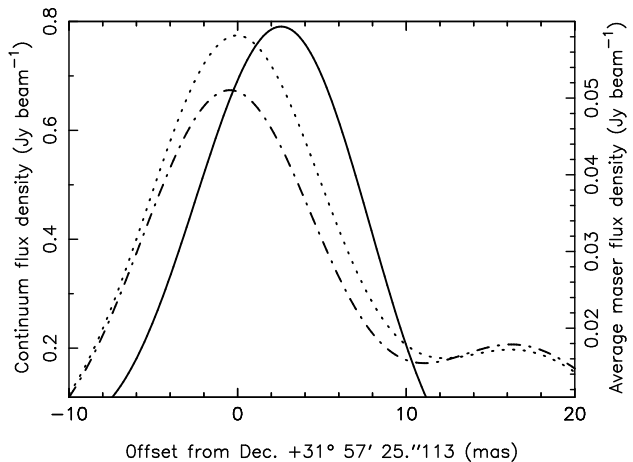
Peak	R.A.	Dec.	σ_{pos} (mas)	S_p (mJy beam $^{-1}$)	σ_{rms} (mJy beam $^{-1}$)
S	00 ^h 48 ^m 47 ^s .14575	+31° 57' 25".1128	0.2	744	6
N	00 ^h 48 ^m 47 ^s .14552	+31° 57' 25".1470	0.4	239	6
\bar{M}	00 ^h 48 ^m 47 ^s .14580	+31° 57' 25".1155	0.7	24 – 107	8


Figure 2. H₂O maser emission from Mrk 348 is shown by the contours, at $(-1, 1, 2, 3, 4\dots)\times 20$ mJy beam $^{-1}$. The grey scale shows continuum emission from 0 to 1 Jy beam $^{-1}$. The circular restoring beam of 12 mas FWHM is shown in the top left panel. The white crosses show the continuum peaks N and S, size proportional to the peak flux. The axes are labelled in mas offset from S. Each panel is labelled with the V_{LSR} (radio convention).

21888.60 MHz, the continuum+line channels from 21890.85 to 21899.10 MHz and line-only channels from 21890.85 to 21899.10 MHz were averaged from their respective data cubes. Flux measurements along slices through these averaged maps, at constant R.A., 2 mas wide, intersecting the position of S, are plotted in Fig. 3. This shows the offset of the maser peak from the brighter continuum peak.

4 DISCUSSION

These observations are the first direct detection of molecular material in the nuclear region of Mrk 348. The existence of H₂O implies shielding by a dusty medium with a col-


Figure 3. Flux density as a function of position along slices through the maser and continuum peaks. The dot-dashed line shows the slice taken from the average of continuum-only channel maps. The dotted line shows the average of channel maps containing maser and continuum emission. The solid line shows the averaged maser emission in these channels after continuum subtraction, note the different flux scale.

umn density $\gtrsim 10^{26} - 10^{27}$ m $^{-2}$ and the conditions required for population inversion of the maser include a gas number density $\sim 10^{14} - 10^{16}$ m $^{-3}$, a fractional abundance of H₂O $\sim 10^{-5} - 10^{-4}$ and a temperature > 250 K (Kartje et al. 1999). Conditions can be more tightly constrained depending on the association of the masers with a disc or a jet.

We assume that the brightest 22-GHz continuum component S contains the core and 2-mas northern jet at position angle 15° found by Ulvestad et al. (1999) at 15 GHz. N is in a similar direction to the more extended jet detected at 1.4 and 5 GHz (Neff & de Bruyn A G 1983; Unger et al. 1984).

We consider three possible models for the relationship between the maser flare and the continuum flare:

- (i) The masers trace a small warped disc and the maser emission follows a Keplerian rotation law, and the masers directly amplify the continuum emission.
- (ii) The masers are unsaturated and lie in a symmetric Keplerian nuclear disc. Perturbation of the disc creates spiral shocks (Maoz & McKee 1998) that are also responsible for the continuum flare.
- (iii) The radio continuum flare is associated with the ejection of material in the direction of the northern jet. The masers arise from the ISM where it is shocked by the jet.

Below we expand on the models and explain why we prefer or reject each.

The ratios of the peak fluxes April:May are 27:77 at 4604 km s $^{-1}$ and 26:107 at 4544 km s $^{-1}$, a 3 – 4-fold increase.

Although further observations are essential in order to pin down the source timescale, such rapid variability may suggest that the individual masing clouds are less than 1 light-month (0.025 pc) in diameter. This would then be about half the size of the 15-GHz core (Ulvestad et al. 1999) and so the maser emission that is beamed in our direction is compact enough to originate from maser clouds that overlap our line of sight to the core. However the two arrows in Fig. 1 indicate the velocities of the peaks that Falcke et al. (2000) observed and which are close to the peaks in our data, but $\sim 100 \text{ km s}^{-1}$ more redshifted than V_{sys} . Falcke et al. (2000) did not detect any maser emission at $V_{\text{LSR}} < V_{\text{sys}}$. So explanation (1) is inconsistent with a Keplerian disc unless the masing material is infalling. Moreover the maser peak is consistently misaligned with S in every channel in Fig. 2. The 3σ position error boxes for \bar{M} and S (Table 1) are too close to rule out direct maser amplification of the continuum peak, but we consider other geometries are more probable.

Maoz & McKee (1998) found a tendency for the redshifted emission from disc supermasers around AGN to be brighter and explained this using a model of spiral shocks within a Keplerian disc. This mechanism requires perturbation of the disc, which could be connected to the event which caused the continuum flare. Such a disc should be symmetric about the nucleus with a well-defined position-velocity gradient. If it is nearly edge-on the rotation velocity is $V_{\text{max}} - V_{\text{sys}} \approx 200 \text{ km s}^{-1}$. The MERLIN results show the velocity gradient is $\leq 2 \text{ mas in } 111 \text{ km s}^{-1}$ corresponding to a disc radius $\lesssim 1.1 \text{ pc}$. \bar{M} is $0.8 \pm 0.2 \text{ pc}$ north of S. This is consistent with the $\lesssim 2 \text{ yr}$ time-lag between detection of the maser and continuum flares which implies a separation of $\lesssim 0.6 \text{ pc}$ (Falcke et al. 2000). This implies that if the masers lie in a symmetric disc it is elongated north-south, parallel to the radio jets. This is unlikely and so model (2) is also improbable.

Model (3), in which the masers originate in a shock produced by the northern jet, is possibly due to the misalignment of the nuclear disc with respect to the host galaxy. If this material was ejected from the core when the continuum flare commenced $\lesssim 2$ years prior to the maser flare this implies speeds near c . The only previous detection of a relativistic Seyfert jet is in III Zw 2 (Brunthaler et al. 2000). However Ulvestad et al. (1999) measured a jet speed of $\sim 0.07c$ for Mrk 348 on similar scales suggesting the jet power is rapidly dissipated once it reaches the shocked region.

If the maser flare is not simply directly amplifying the radio continuum flare this indicates that there is some common excitation effect, possibly some sort of high level nuclear activity. If the masers are found along the radio jets, as is the case for NGC 1052 (Claussen et al. 1998), this mechanism for the correlation between the evolution of the maser flare and the radio flare is an important tool to study the jet-ISM interactions.

We have observed the newly discovered megamaser Mrk 348 with MERLIN at 22 GHz in order to study the masers at higher resolution, test whether there is a correlation between the continuum and maser flux density and investigate their origin in the core or jet, which could give us some more insight to the maser excitation mechanism. Further imaging observations of the whole line will distin-

guish between these possibilities and elucidate the origins of the flare.

5 ACKNOWLEDGEMENTS

We would like to thank our referee Dr. Huib Jan Van Langevelde for many constructive comments. MERLIN is the Multi Element Radio Linked Interferometer Network, a national facility operated by the University of Manchester at Jodrell Bank Observatory on behalf of PPARC. We thank the MERLIN staff for performing the observations, and Peter Thomasson, Simon Garrington and Tom Muxlow for useful discussions. We are grateful to Phil Diamond, Alan Pedlar and Alison Peck for very helpful contributions to this paper. This research was supported by European Commission, TMR Programme, Research Network Contract ERBFMRXCT96-0034 ‘‘CERES’’.

REFERENCES

- Bottinelli L., Gouguenheim L., Fouque P., Paturol G., 1990, *A&AS*, 82, 391
- Braatz J. A., Wilson A. S., Henkel C., 1997, *ApJ*, ApJS, 321
- Brunthaler A., Falcke H., Bower G. C., Aller H., Teräsranta H., Lobanov A. P., Krichbaum T. P., Patnaik A. R., 2000, *A&A*, 357, L45
- Claussen M. J., Diamond P. J., Braatz J. A., Wilson A. S., Henkel C., 1998, *ApJ*, 500, L132
- Cohen R. J., 1998, in Andersen J., ed, *Highlights of Astronomy Vol. 11A*. Kluwer, p. 938
- Condon J. J., Cotton W. D., Greisen E. W., Yin Q. F., Perley R. A., Taylor G. B., Broderick J. J., 1998, *AJ*, 115, 1693
- Elitzur M., Hollenbach D. J., McKee C. F., 1992, *ApJ*, 394, 221
- Falcke H., Wilson A. S., Simpson C., 1998, *ApJ*, 502, 199
- Falcke H., Henkel C., Peck A. B., Hagiwara Y., Almuena Prieto M., Gallimore J. F., 2000, *A&A*, 358, L17
- Gallimore J. F., Baum S. A., O’Dea C. P., Pedlar A., Brinks E., 1999, *ApJ*, 524, 684
- Greisen E., ed, 1994, *AIPS Cookbook*. NRAO, Charlottesville, VA 22903-2475, USA
- Halkides D., Ulvestad J., Roy A., 1997, *BAAS*, 29, 1375
- Huchra J. P., Vogeley M. S., Geller M. J., 1999, *ApJS*, 121, 287
- Kartje J. F., Königl A., Elitzur M., 1999, *ApJ*, 513, 180
- Maoz E., McKee C. F., 1998, *ApJ*, 494, 218

- Miller J. S., Goodrich R. W., 1990, *ApJ*, 355, 456
- Miyoshi M., Moran J., Hernstein J., Greenhill L., Nakai N., Diamond P., Inoue M., 1995, *Nat*, 373, 127
- Neff S. G., de Bruyn A. G., 1983, *A&A*, 128, 318
- Richards A. M. S., Yates J. A., Cohen R. J., 1999, *MNRAS*, 306, 954
- Simkin S. M., van Gorkom J., Hibbard J., Hong-Jun S., 1987, *Science*, 235, 1367
- Simpson C., Mulchaey J. S., Wilson A. S., Ward M. J., Alonso-Herrero A., 1996, *ApJ*, 457, L19
- Ulvestad J. S., Wrobel J. M., Roy A. L., Wilson A. S., Falcke H., Krichbaum T. P., 1999, *ApJ*, 517, L81
- Unger S. W., Pedlar A., Neff S. G., de Bruyn A. G., 1984, *MNRAS*, 209, 15p
- Warwick R. S., Koyama K., Inoue H., Takano S., Awaki H., Hoshi R., 1989, *PASJ*, 41, 739
- Wilkinson P. N., Browne I. W. A., Patnaik A. R., Wrobel J. M., Sorathia B., 1998, *MNRAS*, 300, 790

This paper has been produced using the Royal Astronomical Society/Blackwell Science \LaTeX style file.